Journal of Geochemical Exploration xxx (2008) xxx-xxx

Contents lists available at ScienceDirect

Journal of Geochemical Exploration

journal homepage: www.elsevier.com/locate/jgeoexp

Water management for acid mine drainage control at the polymetallic Zn–Pb–(Ag–Bi–Cu) deposit Cerro de Pasco, Peru

Bernhard Dold [a,*], Cheikh Wade [b], Lluis Fontboté [b]

[a] Centre d'Analyse Minérale, Institute of Mineralogy and Geochemistry, University of Lausanne, CH-1015 Lausanne, Switzerland
[b] Department of Mineralogy, University of Geneva, Rue des Maraîchers 13, CH-1205 Geneva, Switzerland

ARTICLE INFO

Article history:
Received 10 January 2008
Accepted 14 May 2008
Available online xxxx

Keywords:
Sulfide oxidation
Tailings
Waste-rock dump
Cemented zone
Hydrology
Sequential extraction

ABSTRACT

The geochemical and mineralogical study of the Quiulacocha tailings impoundment has shown that the hydrological connection of the three studied mine-waste systems at Cerro de Pasco (Pyrite-rich waste-rock dump Excelsior, old tailings impoundment Quiulacocha, and the active tailings impoundment Ocroyoc) is a critical concern for effective acid mine drainage (AMD) control and mine-waste management. The Quiulacocha tailings covered 114 ha, comprising 79 Mt of tailings, which contained ~50 wt.% pyrite, and are located at 4340 m altitude in a tropical puna climate with about 1025 mm/a rainfall and 988 mm/a of evaporation. The tailings were partially overlain by the Excelsior waste-rock dump, which contains about 26,400,000 m^3 of waste rocks that cover 94 ha and contained ~60 wt.% of pyrite, which origin from a massive pyrite-quartz replacement body. Therefore, these two mine-waste deposits had a direct hydrological connection, resulting in the export of AMD produced at Excelsior towards Quiulacocha. In the Quiulacocha impoundment there are two different types of tailings recognized, that interact with the AMD from Excelsior: 1) Zn–Pb-rich tailings and 2) Cu–As-rich tailings. During the sampling, the Zn–Pb-rich part of Quiulacocha was not producing important excesses of AMD from the oxidation zone, since the pH increased to near neutral values at 1 m depth. The underlying tailings were still able to neutralize the acidity produced in the oxidation zone through sulfide oxidation by the carbonates (mainly dolomite and siderite) contained in the Zn–Pb mineral assemblage. The main source of AMD in this mine-waste system is the Excelsior waste-rock dump. Its acid seepage infiltrates into Quiulacocha forming a Fe–Zn–Pb plume with a pH 5.5–6.1 and containing up to 7440 mg/L Fe, 627 mg/L Zn, and 1.22 mg/L Pb. The plume was detected at 10–13 m depth in the stratigraphy of Quiulacocha tailings. Additionally, the AMD seepage outcropping at the base of the Excelsior waste-rock dump was channeled on the tailings surface into the Quiulacocha pond (pH 2.3), which covered the Cu–As-rich tailings. Infiltration of this Fe(III)-rich AMD increased tailings oxidation in the southwestern part of the impoundment, and subsequently liberated arsenic by enargite oxidation. Additionally, the AMD collected in the Quiulacocha pond was pumped into the active Ocroyoc tailings impoundment, where sulfide oxidation was strongly enhanced by the input of dissolved Fe(III). Therefore, the AMD management and a hydrological separation of the different mine-waste systems could be a first step to prevent further extension of the AMD problem in order to prevent increased sulfide oxidation by Fe(III)-rich solutions.

1. Introduction

There is no doubt that metal production has been and will continue to be in the future a key parameter for the development and wealth of a modern society. However, metal production produces important environmental impacts on other vital resources, especially the formation of metal-loaded acid solutions resulting from sulfide and coal mining, better known as acid mine drainage (AMD) or acid rock drainage (ARD), which are classified by the United States Environmental Protection Agency (EPA) as one of the three top ecological-security threats in the world. Although in the last decades AMD received a great deal of attention from the scientific community (e.g. Nordstrom, 1982; Singer and Stumm, 1970 and references therein), only a few, scarce studies focus on the geochemical processes occurring in the very early stage of AMD formation at active mine sites in order to prevent its formation (e.g. Smuda et al., 2006). Especially, the management of the Fe(III)-rich solution in an active mine site has not received the necessary attention, even when Fe(III) is known as an extremely efficient oxidant especially for sulfide minerals like pyrite, which are not acid soluble (Schippers, 2007).

To fill this gap, we present here a detailed mineralogical and geochemical study of the inactive Quiulacocha and the active Ocroyoc

* Corresponding author. Actual Address: Instituto de Geologia Economica Aplicada (GEA), Universidad de Concepción, Victor Lamas 1290, Concepción, Chile. Tel.: +56 41 2204875; fax: +56 41 2241045.
E-mail addresses: Bernhard.Dold@unil.ch, bdold@udec.cl (B. Dold), wadekheuch@yahoo.fr (C. Wade), Lluis.Fontbote@terre.unige.ch (L. Fontboté).

0375-6742/$ – see front matter © 2008 Elsevier B.V. All rights reserved.
doi:10.1016/j.gexplo.2008.05.002

tailings impoundments at Cerro de Pasco, Peru in order to highlight the geochemical processes taking place in each mine-waste deposit (tailings, waste-rock dump) and the effects resulting from the transfer of AMD through a hydrological connection between the different mine-waste systems impacting on the overall water quality in this setting. The effect of acidity export by AMD from one waste-rock system to another should be taken into account in any mine setting in order to prevent negative geochemical side effects, and Cerro de Pasco is only a good example to highlight these effects. In the frame of this project, different mine-waste types present at the Cerro de Pasco mine, such as for example the waste-rock dump Excelsior (Smuda et al., 2007) and the acid lake Yanamate (Wisskirchen et al., 2005), were studied and published elsewhere.

1.1. Ore geology and deposition history at Cerro de Pasco

The material for both tailings impoundments and the Excelsior waste-rock dump (Fig. 1) originate from the polymetallic Zn–Pb–(Ag–Bi–Cu) deposit at Cerro de Pasco, Peru (Einaudi, 1977; Baumgartner, 2007; Baumgartner et al., in press). The ore is rich in pyrite (FeS_2) and sulfides are the main base-metal carrier. Three different types of ore have been exploited in the history of the mine. In early Spanish colonial times (Cerro de Pasco was founded in 1578 as a miner camp) silver veins were exploited at Cerro de Pasco, transforming it into the mining centre of Peru and one of the most important silver producers in the world at this time. During the first decades of the 20th century, a copper mineralization dominated by chalcopyrite ($CuFeS_2$) associated with enargite (Cu_3AsS_4) was mined. The flotation plant for the Cu ore was located in the southwestern (SW) part of the Quiulacocha tailings impoundment (Figs. 1 and 2), where the tailings were directly deposited in the depression of the natural Quiulacocha lake. From around 1947 the exploitation of Pb–Zn bodies (galena, PbS, and sphalerite ZnS) replacing carbonates (mainly dolomite, $CaMg(CO_3)_2$ and siderite, $FeCO_3$) from the Pucará group (Baumgartner, 2007; Baumgartner et al., in press) was favored and a new flotation plant was built close to the open pit. Therefore, the discharge and deposition point was moved to the north-eastern (NE) part of the tailings, which was closer to the flotation plant.

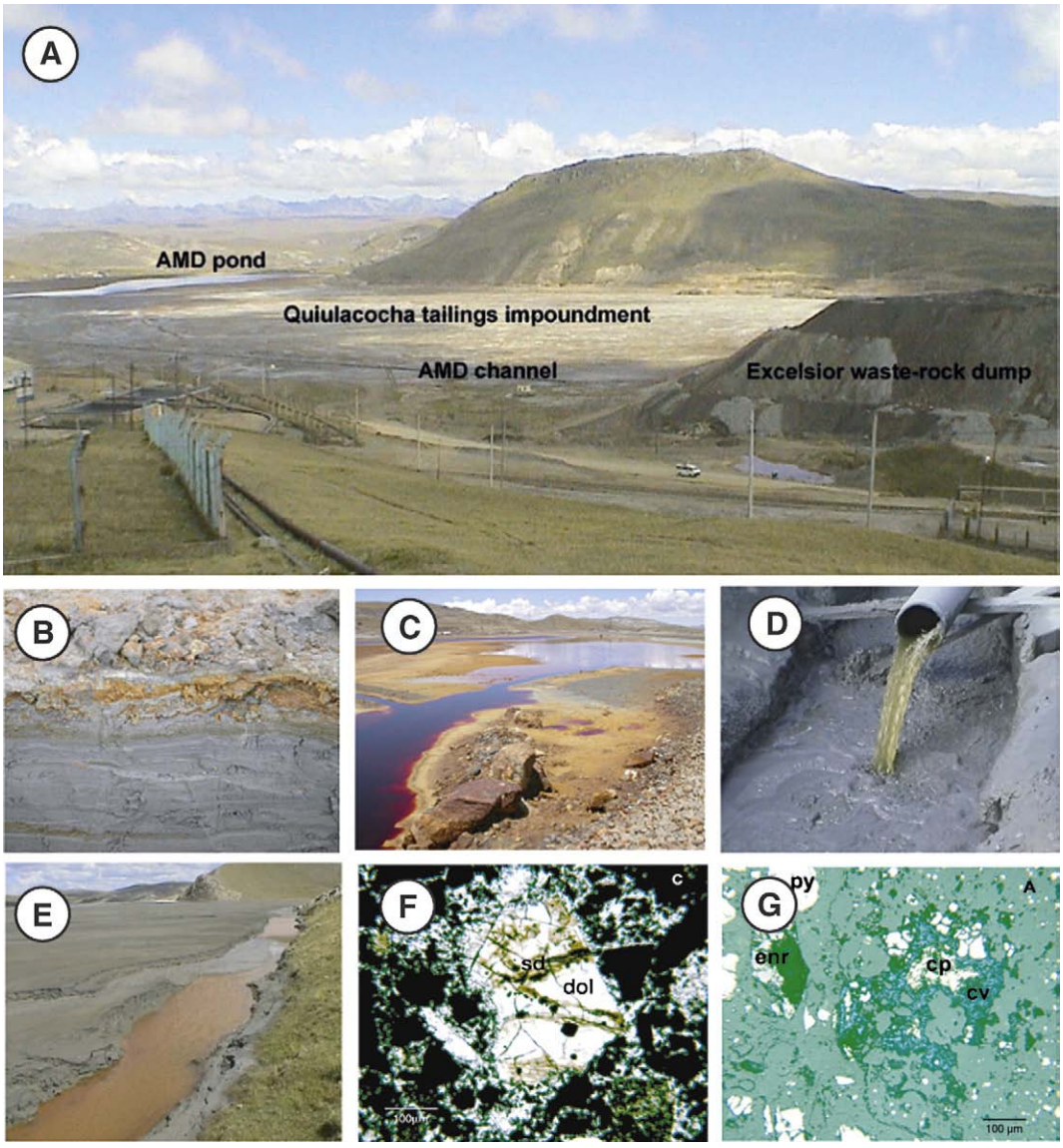

Fig. 1. A) Overview of the Quiulacocha tailings impoundment with the overlying Excelsior waste-rock dump on the right and the acid mine drainage (AMD) pond in the southwestern part of the tailings impoundment. B) 2 cm thin oxidation zone ("cemented zone") after 11 years of oxidation. Profile depth was 10 cm. C) AMD pond in the southwestern part (pH 2.3). D) Input of Fe(III)-rich AMD from the Quiulacocha pond into the alkaline tailings before the deposition in the active tailings impoundment Ocroyoc. E) Active Ocroyoc tailings impoundment with hydrolysis of Fe(III) hydroxides during operation. F) Secondary replacement of dolomite by siderite in the Zn–Pb-rich tailings (CPQ/B 1.5 m). Secondary replacement of chalcopyrite by covellite in the Cu-rich tailings (CPQ/D 9.5 m). Abbreviations: py = pyrite, cp = chalcopyrite, cv = covellite, enr = enargite, sd = siderite, dol = dolomite.

Please cite this article as: Dold, B., et al., Water management for acid mine drainage control at the polymetallic Zn–Pb–(Ag–Bi–Cu) deposit Cerro de Pasco, Peru, Journal of Geochemical Exploration (2008), doi:10.1016/j.gexplo.2008.05.002

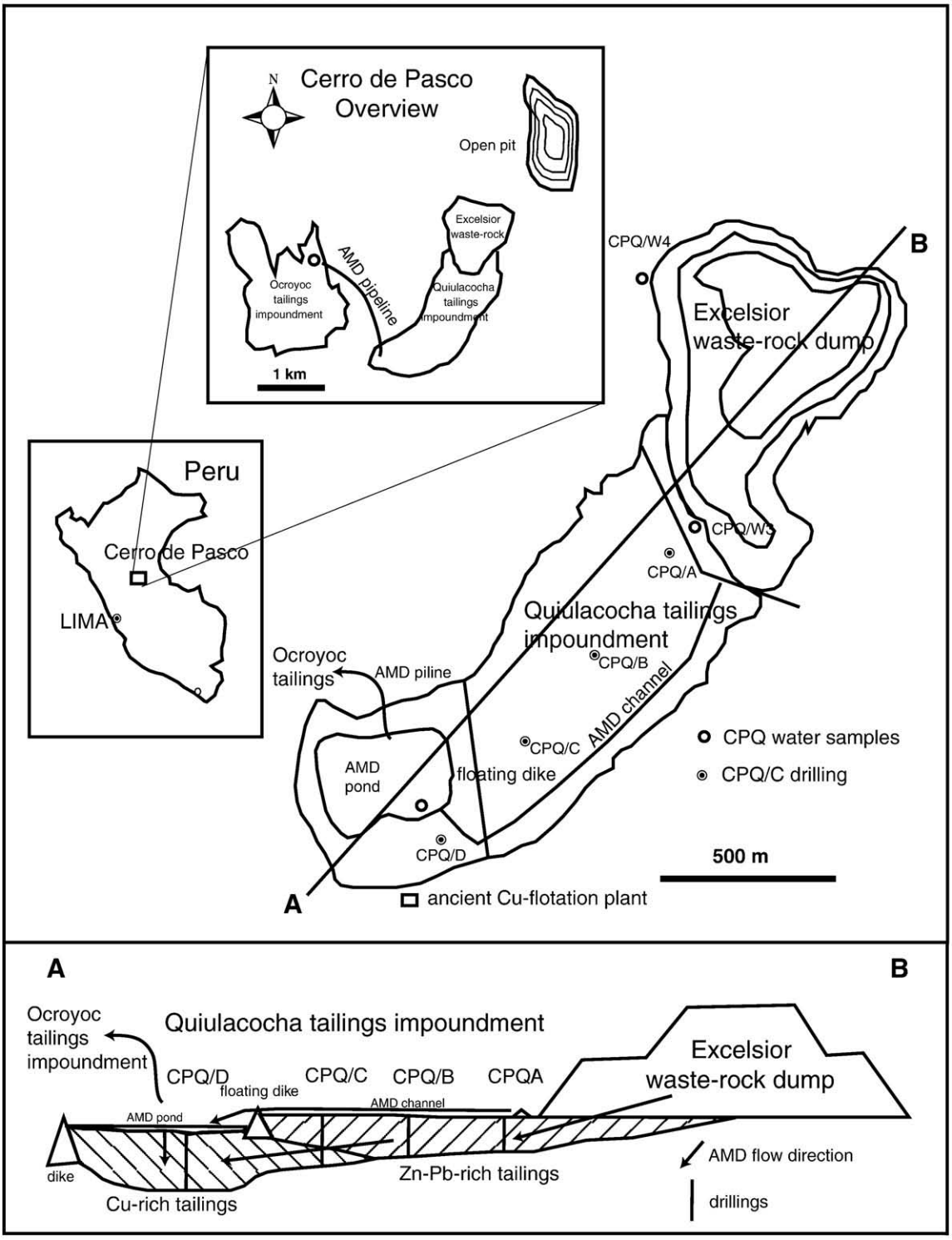

Fig. 2. Location map of the open pit, waste-rock dump and tailings impoundments at Cerro de Pasco, Peru. The Quiulacocha tailings impoundment and the overlaying Excelsior waste-rock dump at Cerro de Pasco are shown in detail. The profile shows the hydrological connection between the two systems, location of drillings, and the distribution of Cu–As-rich and Zn–Pb-rich tailings in the impoundment. The vertical scale of the profile is exaggerated for better visibility.

Due to this deposition history, the Cu tailings are now found in the SW part of Quiulacocha, in the former natural lake of Quiulacocha underlying the Zn–Pb tailings in the central part of Quiulacocha, which were separated by a floating dike (Figs. 1 and 2).

Quiulacocha is located at 1.5 km S–SW of the mine, 170 km N–NE of Lima at an altitude of 4340 m. The tailings are exposed to a humid climate ("tropical puna"; ~1025 mm/y rainfall and ~988 mm/y evaporation). Tailings depositing at Quiulacocha stopped in 1992 after 50 years of operation. The Quiulacocha tailings (114 ha, 79 Mt tailings with ~50 wt.% pyrite) are partially overlain by the Excelsior waste-rock dump (Figs. 1A and 2), which contains about 26,400,000 m^3 of pyrite-rich waste rocks (94 ha, ~60 wt.% of pyrite; Smuda et al., 2007), largely from a pyrite-quartz replacement body located at the western part of the open pit. The active Ocroyoc tailings impoundment is located 7 km SW of the Cerro de Pasco mine (Figs. 1E and 2). During the sampling period in June 2003, the three mine-waste systems were

Please cite this article as: Dold, B., et al., Water management for acid mine drainage control at the polymetallic Zn–Pb–(Ag–Bi–Cu) deposit Cerro de Pasco, Peru, Journal of Geochemical Exploration (2008), doi:10.1016/j.gexplo.2008.05.002

hydrologically connected. Acid mine drainage (AMD) seeping from the base of the Excelsior waste-rock dump was collected and conducted into a channel at the surface of the Quiulacocha tailings towards the AMD pond on the SW part of the tailings impoundment (Figs. 1A, C and 2). Field observations suggest that a significant amount of the AMD from the Excelsior waste-rock dump infiltrates into Quiulacocha tailings. The excess AMD (pH 2.3; Fig. 1C), which was collected in the pond, was pumped into the active Ocroyoc tailings, where it mixed with the alkaline tailings (pH 11.3) from the flotation plant (Fig. 1D).

2. Sampling and analytical methods

2.1. Field sampling

From the Quiulacocha tailings impoundment 88 solid samples were obtained by flush drilling to a maximum depth of 26 m at 4 locations (CPQ/A, CPQ/B, CPQ/C, CPQ/D; Fig. 2) during the field campaign in May–June 2003. The drillings crossed the whole stratigraphy of the Quiulacocha tailings to the basement of Devonian shales and phyllites (Fig. 2). A detailed study of the oxidation zone was conducted by surface sampling at 7 locations. To sample the pore-water, 3 inch diameter aluminum tubes were used for coring at several depths of the drillings and were quickly frozen (−20 °C) until pore-water extraction. The pore-water (8 samples) was obtained by replacement with epoxidized soybean oil (PARAPLEX®) in the laboratory as modified following the method described by Patterson et al. (1978). The surface waters of the Quiulacocha and Ocroyoc pond were sampled and analyzed. The data for the two AMD outgroppings at Excelsior (CPE-W3 and CPE-W4) were cited from Smuda et al. (2007). Water and pore-water pH, Eh, and alkalinity were measured immediately during water sampling or pore-water extraction. The pH electrodes were calibrated with pH 4 and 7 standard solutions. The performance of the Eh electrodes were controlled by Zobell's (Nordstrom, 1977) and Light's (Light, 1972) solutions and Eh values were corrected to the standard hydrogen electrode (SHE). All water samples were filtered through 0.2 µm regenerated cellulose and stored at +4 °C in the dark prior to analysis. Samples for cation analyses were acidified to pH<2 with suprapure HNO_3. During solid sampling, pH was measured with a WTW pH-meter (WTW pH 323) with a special pH-electrode (WTW-Sentix RP) inserted directly into the moist tailings.

2.2. Mineralogy and geochemistry of the solids

The mineralogical study included thin and polished section microscopy, SEM-EDS (JOEL 6400) studies, X-ray diffraction (Philips 3020) and differential X-ray diffraction (DXRD; Dold, 2003a). Selected solid samples (39) were analyzed by X-ray fluorescence (Philips PW 2400). Sixteen samples were subjected to a seven-step sequential extraction procedure described by Dold (2003b), where step 1 releases the water-soluble fraction (1.0 g sample into 50 ml deionized H_2O shaken for 1 h at room temperature RT); step 2 releases the exchangeable fraction (1 M NH_4-acetate, pH 4.5, shaken for 2 h, RT); step 3 addresses the Fe(III) oxyhydroxides fraction (0.2 M NH_4-oxalate, pH 3.0, shaken for 1 h in darkness, RT); step 4 dissolves the Fe(III) oxides fraction (0.2 M NH_4-oxalate, pH 3.0, heat in water bath 80 °C for 2 h); step 5 consists of a change from a reducing to an oxidizing condition and is performed by a H_2O_2 leach (35% H_2O_2 heat in water bath for 1 h) dissolving secondary sulfide minerals like covellite; step 6 ($KClO_3$ and HCl, followed by 4 M HNO_3 boiling) dissolves primary sulfides and step 7 (HCl, HF, $HClO_4$, HNO_3) consists in the residual fraction (silicates). The leaches were analyzed by ICP-AES at the SGS Laboratory, Toronto, Canada.

2.3. Water analysis

The 10 water samples (2 surface and 8 pore-water samples) were analyzed by ICP-MS (Perkin Elmer HP 4500 Series 100) and major cations and anions by ion chromatography (Dionex DX 120).

2.4. Pore gas composition

O_2, CO_2, and H_2S concentrations in the pore gas of the unsaturated zone were measured by a Dräger® Multiwarn II portable analyzer.

3. Results and discussion

3.1. Hydrology and AMD characteristics

The hydrological situation was characterized by strong water seepage from the Excelsior waste-rock dump towards the Quiulacocha tailings impoundment visible by AMD outcropping at the base of the

Table 1
Hydrochemical data from the pond waters from Quiulacocha and Ocroyoc and the pore waters from the drillings CPQ/A, CPQ/B, CPQ/C, and CPQ/D

Samples		pH	Ion chromatography										ICP-MS					
			Anions				Cations											
			F (mg/L)	CL (mg/L)	NO_3 (mg/L)	SO_4 (mg/L)	Li (mg/L)	Na (mg/L)	K (mg/L)	NH_4 (mg/L)	Mg (mg/L)	Ca (mg/L)	Al (mg/L)	Fe (mg/L)	Cu (mg/L)	Zn (mg/L)	As (mg/L)	Pb (mg/L)
Tailings ponds																		
Quiulacocha pond		2.3	BDL	85.5	BDL	44,424	BDL	111	63	BDL	4032	900	56.7	1691	26.9	578	6.54	0.63
Ocroyoc pond		10	BDL	26.3	6.4	1642	BDL	50.8	15.5	2	BDL	974	0.16	3.63	0.03	1.09	0.1	0.52
Porewater drillings																		
CPQ/A	50 cm	3.4	2	13.9	BDL	1791	BDL	27.8	17.8	2.2	BDL	BDL	0.07	3.51	0.03	0.65	0.12	0.18
	4.7 m	5.4	1.9	19.2	BDL	3779	BDL	31	BDL	BDL	243	825	0.39	96.1	0.03	4.18	0.55	0.74
CPQ/B	50 cm	3.3	BDL	BDL	BDL	3204	BDL	50.2	18.7	2.4	215	634	0.27	65.0	0.06	6.56	0.12	0.76
	10 m	6.1	BDL	BDL	BDL	5582	BDL	23	27	22	1742	507	0.23	1262	0.03	153	0.25	1.12
	16.7 m	6.4	BDL	BDL	BDL	813	BDL	35.3	16.9	12.9	115	853	0.16	145	0.05	2.54	0.57	0.85
CPQ/C	50 cm	3.7	BDL	17.6	BDL	21,336	BDL	31.3	30.6	8.2	1424	408	0.18	58.9	0.04	3.87	0.16	0.23
	13 m	5.5	BDL	BDL	BDL	20,010	BDL	5.6	5	BDL	247	857	2.19	7440	0.03	627	0.45	1.22
CPQ/D	50 cm	–	–	–	–	–	BDL	8.5	2.5	3.6	10.4	234	8.74	10,890	2.04	633	2.08	1.69
AMD from Excelsior[a]																		
CPE-W3[a]		5.1	–	–	–	29,190	–	8.2	27.7	–	4716	694	–	5640	1.28	2302	1.98	1.28
CPE-W4[a]		2.8	–	–	–	29,400	–	BDL	3.1	–	7792	614	–	1632	161	3000	7.99	0.14

[a]The AMD data from Excelsior were all measured by ICP-AES and taken from Smuda et al. (2007).
– not measured.
BDL=below detection limit.

Please cite this article as: Dold, B., et al., Water management for acid mine drainage control at the polymetallic Zn–Pb–(Ag–Bi–Cu) deposit Cerro de Pasco, Peru, Journal of Geochemical Exploration (2008), doi:10.1016/j.gexplo.2008.05.002

Table 2
Semi-quantitative mineralogical compositions of representative samples from the four drillings and surface samples from the oxidation zone

Drilling	Ore type	Sample	Depth (m)	Paste-pH	Zone	py/mr	gn	sl	po	cp	enr	cv	hm	dol	sd	qtz	jt	gy	gt & HFO
CPQ/A	Zn–Pb tailings	CPQ.1	0.05	3.3	OZ	XXX		X								XX	XX	XXX	XXXX
CPQ/A		CPQ.8	0.08	4.0	OZ	XXX	X		X						X	XX	XX	XXX	XX
CPQ/A		CPQ8	0.43	6.9	PZ	XXXX	X	XX	X			X	X	X	XX	XX		X	
CPQ/A		CPQ/A.5.4	5.4	5.8	PZ	XXXX	XX	XX	XX					X	XX	XX		X	
CPQ/A		CPQ/A10.5	14.9	6.3	PZ	XXXX	XX	XX	XX					X	XX	XX		X	
CPQ/B		CPQ/B 0.05	0.05	3.4	OZ	XXX	X	X								XX	XX	XXX	XXX
CPQ/B		CPQ/B 0.5	0.5	6.3	PZ	XXXX	XX	XX						X	X	XXX		XX	
CPQ/B		CPQ/B 5.5	5.5	7.8	PZ	XXXX	XX	XXX						XX	XX	XXX		X	
CPQ/B		CPQ/B 25.7	25.7	6.2	PZ	XXXX	XX	XX						XXX	X	XXX		X	
CPQ/C		CPQ/C 2.5	2.5	8.3	PZ	XXXX	XX	XX						XX	XX	XXX		X	
CPQ/C		CPQ/C 4.5	4.5	8.3	PZ	XXXX	X							XXX	XX	XXX		X	
CPQ/D	Cu tailings	CPQ/OZ	0.06	3.0	OZ	XXX										XXX	XX	XX	XX
CPQ/D		CPQ/D 3.5	3.5	5.4	PZ	XXXX	X	X		XXX	XXX	X				XX			
CPQ/D		CPQ/D 9.5 A	8.5	3.7	PZ	XXXX	X	X		XX	XX	X				XX			
CPQ/D		CPQ/D 9.5 B	9.5	4.1	PZ	XXXX				XX	XX	XXX				XX			

Abbreviations: py:pyrite, mr: marcassite, gn: galena, sl: sphalerite, po: pyrrhotite, cp: chalcopyrite, enr: enargite, h hematite, dol: dolomite, cv: covellite, sd: siderite, qtz: quartz, jt: jarosite, gy: gypsum, gt: goethite, HFO: Fe(III) hydroxyde. OZ: oxidation zone, PZ: primary zone.

Excelsior waste-rock dump. Smuda et al. (2007) could detect two different types of AMD at Excelsior. In the northern part of the waste dump, Cu-, Cd-, and As-rich acid solution, most likely originating from waste material produced when mining activity began, and the arsenic rich Cu-sulfide ore with enargite was exploited (CPE-W4: pH of 2.78, conductivity of 26.0 mS/cm, Eh of 684 mV, 29,600 mg/L SO_4^{2-}, 1632 mg/L Fe, 6.66 mg/L Cd, 3000 mg/L Zn, 161 mg/L Cu, 0.14 mg/L Pb, 7.99 mg/L As; Table 1). In the southern part less acidic AMD seeped from the waste dump, most likely controlled by the ore's Zn–Pb mineralogy (CPE-W3: pH of 5.1, conductivity of 23.3 mS/cm, Eh of 319 mV, 29,390 mg/L SO_4^{2-}, 5640 mg/L Fe, 3.58 mg/L Cd, 2302 mg/L Zn, 1.28 mg/L Cu, 1.28 mg/L Pb, 1.98 mg/L As). These seepages resulted in a nearly complete water saturation of the Quiulacocha tailings. The groundwater level was close to the surface (0–10 cm depth) near the

Table 3
XRF and paste-pH data for representative samples from the four drillings in Quiulacocha

	Depth (m)	Paste-pH	SiO_2 (wt.%)	Al_2O_3 (wt.%)	MnO (wt.%)	CaO (wt.%)	MgO (wt.%)	K_2O (wt.%)	TiO_2 (wt.%)	Fe (wt.%)	S (wt.%)	Zn (wt.%)	Pb (wt.%)	As (wt.%)	Cu (wt.%)
CPQ/A	0.05	3.3	25.05	0.71	0.56	0.86	0.16	0.08	0.02	22.65	47.86	1.04	0.49	0.17	0.02
CPQ/A	2.50	–	20.14	1.19	1.59	0.67	1.30	0.06	0.03	26.33	45.97	1.38	0.54	0.16	0.04
CPQ/A	4.20	–	17.21	0.60	0.80	0.30	0.55	0.01	0.01	21.37	52.55	4.22	0.61	0.14	0.04
CPQ/A	5.40	5.8	16.74	0.49	0.55	0.25	0.36	0.01	0.01	22.48	55.76	1.90	0.51	0.13	0.03
CPQ/A	8.90	6.2	14.05	0.59	2.33	0.76	9.23	0.05	0.03	20.58	47.66	2.32	0.81	0.12	0.06
CPQ/A	10.70	5.8	25.72	0.74	0.77	0.93	0.55	0.05	0.01	21.71	47.84	0.78	0.36	0.17	0.03
CPQ/A	11.00	–	24.85	0.61	1.90	0.17	1.05	0.04	0.00	32.85	47.57	7.65	0.55	0.24	0.05
CPQ/A	11.70	5.8	23.28	0.49	0.85	0.50	1.09	0.03	0.02	21.37	50.95	0.49	0.39	0.15	0.03
CPQ/A	12.40	–	20.31	0.19	0.73	0.19	0.39	0.01	0.01	23.85	52.74	0.83	0.30	0.11	0.04
CPQ/A	13.90	6.1	19.57	0.66	0.86	0.38	0.81	0.02	0.02	22.32	52.19	1.82	0.48	0.17	0.05
CPQ/A	15.70	5.8	25.10	0.84	1.54	1.10	0.82	0.06	0.03	20.17	47.49	0.82	0.32	0.12	0.06
CPQ/B	1.50	7.7	24.01	2.41	2.10	1.87	0.94	0.15	0.05	27.08	14.02	1.40	0.47	0.16	0.02
CPQ/B	2.50	8.1	24.55	1.81	2.67	1.37	0.90	0.14	0.03	28.65	12.54	1.08	0.39	0.16	0.02
CPQ/B	3.50	8.3	23.37	4.37	2.16	1.82	1.38	0.21	0.06	26.64	11.96	0.79	0.51	0.14	0.03
CPQ/B	6.50	7.9	18.51	1.83	1.37	0.77	0.38	0.07	0.03	28.86	17.74	0.85	0.48	0.17	0.04
CPQ/B	7.50	7.4	34.45	2.97	0.99	1.93	0.46	0.16	0.05	21.57	13.72	1.36	0.51	0.13	0.05
CPQ/B	8.50	7.3	32.73	4.09	1.10	1.56	0.93	0.19	0.08	20.50	12.97	1.23	0.82	0.16	0.06
CPQ/B	9.50	6.1	35.63	4.05	1.40	1.20	0.73	0.21	0.10	19.56	11.89	1.71	1.12	0.18	0.06
CPQ/B	11.00	5.6	32.32	2.04	1.20	1.51	0.85	0.15	0.08	21.67	13.81	1.15	1.09	0.16	0.11
CPQ/B	13.00	5.3	32.26	0.89	0.42	0.79	0.25	0.06	0.05	22.22	17.31	0.77	0.54	0.17	0.04
CPQ/B	17.70	6.7	26.16	2.16	2.42	2.53	2.53	0.13	0.06	22.16	14.52	1.99	0.61	0.19	0.11
CPQ/B	23.70	–	46.98	2.38	0.02	0.41	1.23	0.14	0.14	15.13	13.32	2.17	0.33	0.17	0.19
CPQ/B	24.70	6.3	25.30	1.38	0.03	0.55	1.03	0.08	0.07	22.74	20.24	2.87	0.67	0.31	0.16
CPQ/B	26.70	6.1	26.76	1.33	0.02	0.10	1.21	0.06	0.05	22.19	18.74	3.51	0.08	0.30	0.03
CPQ/C	2.50	8.3	22.10	2.58	2.07	1.36	2.23	0.22	0.03	25.30	41.86	0.91	0.60	0.15	0.03
CPQ/C	3.50	8.3	21.32	2.88	2.50	1.45	2.75	0.20	0.04	28.20	38.62	0.85	0.47	0.13	0.03
CPQ/C	6.50	7.5	25.40	2.31	1.85	1.11	1.08	0.10	0.03	24.41	41.52	0.83	0.63	0.14	0.04
CPQ/C	9.50	–	29.99	1.17	0.94	0.78	1.00	0.06	0.02	20.46	43.84	0.80	0.39	0.20	0.05
CPQ/C	11.50	6.1	23.43	0.79	0.89	0.40	0.35	0.05	0.02	22.42	49.62	0.92	0.54	0.15	0.04
CPQ/C	15.00	5.4	17.70	1.76	1.02	0.47	1.08	0.05	0.02	23.10	53.39	1.25	0.50	0.20	0.05
CPQ/C	18.00	6.1	26.07	0.41	2.52	0.50	8.49	0.03	0.02	26.84	48.06	3.79	0.69	0.25	0.12
CPQ/C	20.00	6.3	25.84	1.76	1.39	1.08	1.25	0.11	0.05	20.66	45.87	0.61	0.60	0.17	0.06
CPQ/C	24.00	6.1	32.55	1.05	0.34	0.65	0.22	0.05	0.04	17.06	44.99	1.43	0.51	0.16	0.20
CPQ/D	3.50	5,3	28.44	7.02	0.67	0.90	0.36	0.62	0.15	19.89	12.42	2.03	2.99	0.33	0.15
CPQ/D	4.50	5.4	26.00	5.46	0.74	1.19	0.37	0.32	0.10	22.08	14.63	1.58	2.18	0.27	0.15
CPQ/D	5.50	6.1	27.13	5.09	0.87	1.80	0.50	0.27	0.09	21.65	13.83	1.62	1.54	0.15	0.10
CPQ/D	6.50	5.8	25.34	4.89	1.83	1.84	0.62	0.26	0.10	23.32	12.78	1.44	1.49	0.26	0.16
CPQ/D	8.50	4.8	30.63	4.75	0.79	1.84	0.62	0.35	0.13	18.00	14.17	1.66	1.87	0.19	0.14
CPQ/D	9.50	4.1	43.89	3.19	–	0.07	–	0.08	0.08	15.20	14.30	0.17	0.46	0.16	0.58

– not measured.

Please cite this article as: Dold, B., et al., Water management for acid mine drainage control at the polymetallic Zn–Pb–(Ag–Bi–Cu) deposit Cerro de Pasco, Peru, Journal of Geochemical Exploration (2008), doi:10.1016/j.gexplo.2008.05.002

Table 4
Results form sequential extraction: Fe-1: water-soluble fraction; Fe-2: exchangeable fraction (NH_4-acetate); Fe-3: Fe(III) oxyhydroxides fraction (NH_4-oxalate, in darkness, RT); Fe-4 Fe(III) oxides fraction (NH_4-oxalate, heat in 80 °C); Fe-5: secondary sulfide (H_2O_2 heat); Fe-6: sulfides fraction ; Fe-7 residual fraction (silicates)

Analyte	Fe-1	Fe-2	Fe-3	Fe-4	Fe-5	Fe-6	Fe-7	Fe-total	S-1	S-2	S-3	S-4	S-5	S-6	S-7	S total	Mn-1	Mn-2	Mn-3	Mn-4	Mn-5	Mn-6	Mn-7	Mn total	Zn-1	Zn-2	Zn-3	Zn-4	Zn-5	Zn-6	Zn-7	Zn total	Pb-1	Pb-2	Pb-3
DL	0.01	0.01	0.01	0.01	0.01	0.01	0.01		0.01	0.01	0.01	0.01	0.01	0.01	0.01		2	2	2	2	2	2	2		0.5	0.5	0.5	0.5	0.5	0.5	0.5		2	2	2
Units	wt. %	wt. %	wt. %	wt. %	wt. %	wt. %	wt. %	wt. %	wt. %	wt. %	wt. %	wt. %	wt. %	wt. %	wt. %	wt. %	mg/kg	mg/kg	mg/kg	mg/kg	mg/kg	mg/kg	mg/kg	mg/kg	mg/kg	mg/kg	mg/kg	mg/kg	mg/kg	mg/kg	mg/kg	mg/kg	mg/kg	mg/kg	mg/kg
CPQ/A/0.50	5.57	0.31	2.11	2.45	2.56	13.6	0.33	26.9	5.5	0.22	0.46	0.13	2.65	16.5	0.75	26.21	3450	1060	744	1230	129	19	4	6636	5570	525	378	763	3510	2230	7.8	12,984	61	205	551
CPQ/A/4.20	2.76	0.4	2.6	1.88	1.37	21.4	0.47	30.9	3.09	0.15	0.43	0.05	1.81	22.8	0.87	29.2	2390	821	2830	2580	1140	29	2	9792	13,300	2160	2480	1520	14,900	15,040	91	49,491	235	1840	560
CPQ/A/11.0	1.2	1.88	3.36	2.34	2.63	22.5	0.46	34.4	1.69	1.01	0.93	0.43	2.66	22.9	0.88	30.5	2450	731	505	1330	432	24	3	5475	8620	1430	300	396	931	859	10.5	12,547	4	69	646
CPQ/A/12.4	4.07	0.9	2.43	1.63	3.16	22.6	0.5	35.3	3.2	0.28	0.33	0.06	2.09	21.5	0.87	28.33	1970	932	2420	1360	645	27	2	7356	2730	605	1020	252	1730	2130	19.7	8487	165	834	789
CPQ/A/15.6	0.4	0.41	3.72	1.49	2	20.3	0.56	28.9	1.7	0.28	0.75	0.05	1.74	21.2	1.09	26.81	3570	1030	7050	3810	2580	69	4	18,113	3840	522	1210	490	3950	1720	22.3	11,754	2	341	762
CPQ/B/1.50	0.08	0.12	1.86	1.16	1.67	29.7	0.7	35.3	0.34	0.07	0.14	0.02	1.15	22.7	1.39	25.81	378	188	1870	2100	4720	6190	79	15,525	872	131	694	324	1890	6930	134	10,975	308	1630	550
CPQ/B/9.50	0.14	0.22	2.19	1.48	1.28	20.5	0.71	26.5	0.65	0.16	0.34	0.03	1.14	18.3	1.36	21.98	1080	552	1260	2290	3510	4420	47	13,159	3010	402	1170	808	3380	7610	203	16,583	244	4010	693
CPQ/B/11.0	0.15	0.2	2.19	1.44	1.03	24.3	0.76	30.1	0.84	0.17	0.4	0.04	1.02	20.9	1.47	24.84	1040	453	1150	2280	3050	4210	45	12,228	3250	336	1200	536	2330	6430	136	14,218	228	4720	571
CPQ/B/24.7	0.51	0.12	0.82	0.53	0.99	34.4	1.52	38.9	0.73	0.08	0.21	0.07	0.99	28.1	2.1	32.28	66	11	22	66	13	60	6	244	3390	366	246	595	2640	14,000	866	22,103	212	885	610
CPQ/B/26.7	0.43	0.09	0.97	0.84	1.22	33.3	0.88	37.7	0.65	0.11	0.26	0.08	1.33	27.9	1.8	32.13	25	42	23	153	36	30	4	313	5010	604	799	1240	6800	21,100	948	36,501	253	2060	520
CPQ/C/2.50	0.09	0.52	5.31	2.3	3.18	18.2	0.51	30.1	1.22	0.22	0.98	0.08	1.74	18.3	0.97	23.51	2900	922	5720	2990	6670	634	6	19,842	3030	518	1790	576	3150	1520	20	10,604	5	459	456
CPQ/C/12.0	1.78	0.43	2.68	2	2.15	25.7	0.8	35.5	1.86	0.16	0.5	0.05	1.67	23	1.41	28.65	1730	903	2730	2500	1980	49	4	9896	3810	793	1240	487	4830	3120	30.4	14,310	137	414	683
CPQ/C/24.0	0.7	0.24	2.23	0.93	1.26	22.4	0.63	28.4	1.91	0.18	0.7	0.06	1.34	23	1.42	28.61	1780	501	841	1250	22	27	5	4426	8400	802	841	695	5950	4590	45.1	21,323	49	185	537
CPQ/D/4.50	0.32	0.46	4.22	2.43	1.95	16.4	0.45	26.2	1.42	0.36	0.65	0.18	1.16	17.4	1	22.17	2420	957	465	1560	2920	529	7	8858	6510	459	1980	750	4250	6590	82.1	20,621	204	6440	566
CPQ/D/5.50	0.16	0.32	3.85	1.66	1.5	20.3	0.6	28.4	1.29	0.31	0.57	0.05	1.26	19.5	1.29	24.27	2240	808	715	1820	2750	2180	19	10,532	6410	639	1870	703	4680	7820	145	22,267	206	7160	620
CPQ/D/9.50	0.24	0.03	0.03	0.02	0.62	28.5	0.89	30.3	0.34	0.08	0.02	0.03	0.69	25.4	1.58	28.14	31	<2	3	<2	<2	41	4	79	307	12	25.5	9.1	138	1470	120	2082	305	3070	185

DL=detection limit.

Table 4 (*continued*)

Analyte	Pb-4	Pb-5	Pb-6	Pb-7	Pb total	Cu-1	Cu-2	Cu-3	Cu-4	Cu-5	Cu-6	Cu-7	Cu total	As-1	As-2	As-3	As-4	As-5	As-6	As-7	As total	Cd-1	Cd-2	Cd-3	Cd-4	Cd-5	Cd-6	Cd-7	Cd total	Sr-1	Sr-2	Sr-3	Sr-4	Sr-5	Sr-6	Sr-7	Sr total
DL	2	2	2	2		0.5	0.5	0.5	0.5	0.5	0.5	0.5		3	3	3	3	3	3	3		1	1	1	1	1	1	1		0.5	0.5	0.5	0.5	0.5	0.5	0.5	
Units	mg/kg	mg/kg	mg/kg	mg/kg	mg/kg	mg/kg	mg/kg	mg/kg	mg/kg	mg/kg	mg/kg	mg/kg	mg/kg	mg/kg	mg/kg	mg/kg	mg/kg	mg/kg	mg/kg	mg/kg	mg/kg	mg/kg	mg/kg	mg/kg	mg/kg	mg/kg	mg/kg	mg/kg	mg/kg	mg/kg	mg/kg	mg/kg	mg/kg	mg/kg	mg/kg	mg/kg	mg/kg
CPQ/A/0.50	359	67	2150	509	3902	38.1	10.5	25	1.1	76.4	84.2	1.9	237	16	26	775	606	352	648	16	2439	21	2	<1	<1	10	8	<1	41	49.2	5.8	6.1	10.4	2.3	9.3	242.0	325.1
CPQ/A/4.20	379	32	4610	430	8086	1.4	16.2	15.7	1.6	77.5	359	5.4	477	13	87	590	49	16	1570	23	2348	48	8	2	<1	71	62	<1	191	4.7	7.8	1.5	3.7	3.3	2.1	137.0	160.1
CPQ/A/11.0	292	89	2320	375	3795	114	26	73.1	5.1	196	163	4.9	582	4	269	857	343	192	586	13	2264	34	5	<1	<1	3	3	<1	45	0.7	0.7	1.6	4.2	<0.5	1.5	122.0	130.7
CPQ/A/12.4	128	35	2010	331	4292	29.9	76	50.6	1.5	34.9	464	8.2	665	19	85	491	22	11	1310	19	1957	16	2	1	<1	8	6	<1	33	5.1	3.0	1.9	4.1	1.4	2.2	108.0	125.7
CPQ/A/15.6	312	29	2070	693	4209	47.3	83.7	79	3.9	160	459	9.7	843	<3	50	519	54	97	1250	27	1997	14	3	<1	<1	13	5	<1	35	8.3	1.9	2.0	3.3	5.9	4.9	243.0	269.3
CPQ/B/1.50	98	127	1300	627	4640	13.6	15.9	14.8	1.8	49.5	115	6.9	218	<3	55	240	20	9	1640	29	1993	7	<1	<1	<1	6	25	<1	38	4.3	6.3	<0.5	0.6	2.1	2.2	258.0	273.5
CPQ/B/9.50	712	100	3670	2480	11,909	86.7	37.9	139	3.1	184	264	7.1	722	4	38	702	134	9	1620	43	2550	32	3	2	<1	16	28	<1	81	2.7	6.8	0.7	2.0	2.3	13.5	602.0	630.0
CPQ/B/11.0	617	143	4270	1570	12,119	135	73.3	295	3.4	316	452	10	1285	<3	25	598	149	5	1410	31	2218	49	4	4	<1	20	26	<1	103	4.6	6.0	0.6	1.0	2.0	6.8	462.0	483.0
CPQ/B/24.7	399	53	3520	951	6630	173	20.2	123	36.4	184	1160	295	1992	20	432	1020	306	64	2290	79	4211	12	1	<1	<1	8	65	3	89	2.6	1.4	1.9	3.2	<0.5	<0.5	479.0	488.1
CPQ/B/26.7	429	83	5970	2120	11,435	91.3	14.2	47.4	3.7	52.6	235	29.6	474	22	98	1210	402	49	2510	51	4342	18	2	1	<1	26	113	3	163	1.1	5.0	3.5	10.0	1.6	3.0	783.0	807.2
CPQ/C/2.50	338	18	4010	1190	6476	2.3	29	15.2	0.9	104	161	2.6	315	<3	56	684	113	19	1160	25	2057	15	5	<1	<1	10	3	<1	33	14.7	2.6	2.1	2.4	12.6	11.9	459.0	505.3
CPQ/C/12.0	301	17	4000	529	6081	131	63.4	61.8	3.8	140	333	6.2	739	18	108	868	68	36	1910	44	3052	24	3	1	<1	19	9	<1	56	6.0	3.0	1.4	2.7	3.5	3.3	201.0	220.9
CPQ/C/24.0	944	60	3850	1060	6685	894	93.4	428	45.3	356	1020	22.2	2859	14	110	948	169	139	1260	36	2676	32	3	1	<1	20	17	<1	73	13.0	2.4	7.5	7.3	1.3	8.9	538.0	578.4
CPQ/D/4.50	781	116	10,200	3780	22,087	419	57.9	410	6.2	404	503	5.4	1806	16	25	1800	703	7	985	30	3566	43	3	1	<1	16	24	<1	87	5.6	37.2	1.1	2.4	3.8	17.3	692.0	759.4
CPQ/D/5.50	819	80	3990	3660	16,535	268	70.5	218	2.6	239	290	3.8	1092	<3	9	1050	185	6	1010	30	2290	59	4	1	<1	18	31	<1	113	5.5	12.5	1.3	2.2	4.1	17.5	745.0	788.1
CPQ/D/9.50	52	7	452	765	4836	1160	65.3	122	92.3	1090	3810	885	7225	6	137	80	37	114	1830	145	2349	1	<1	<1	<1	<1	3	<1	4	2.3	5.5	4.9	4.6	<0.5	<0.5	371.0	388.3

Please cite this article as: Dold, B., et al., Water management for acid mine drainage control at the polymetallic Zn–Pb–(Ag–Bi–Cu) deposit Cerro de Pasco, Peru, Journal of Geochemical Exploration (2008), doi:10.1016/j.gexplo.2008.05.002

Excelsior waste-rock dump and at 1 m depth in the area of the floating dike (Fig. 2). The southwestern part with the AMD pond (pH of 2.3, conductivity of 18.7 mS/cm, Eh of 434 mV, 44,424 mg/L SO_4^{2-}, 1691 mg/L Fe, 578 mg/L Zn, 26.8 mg/L Cu, 0.62 mg/L Pb, 6.54 mg/L As) was nearly completely water saturated.

Mineralogical (Table 2) and geochemical data (Tables 3 and 4) from the four drillings (max. 26.7 m depth) showed that two different tailings types can be distinguished in the Quiulacocha tailings stratigraphy: Zn–Pb-rich tailings in the northern part overlying the older, Cu–As-rich tailings, which are present in the southern part of the impoundment (Fig. 2B).

3.2. Zn–Pb-rich sulfidic tailings

The mineralogy of the Zn–Pb-rich sulfidic tailings was characterized by an assemblage of pyrite–sphalerite–galena–pyrrhotite. Gangue minerals were mainly the carbonates dolomite and siderite, although silicates, mainly quartz, were also present. The Zn–Pb-rich tailings represent two-thirds of the tailings surface and were deposited in the NE part, partially overlaying the older Cu tailings (Fig. 2). Due to the tailings deposition process, a grain size fractionation from a coarser grain size close to the Excelsior waste-rock dump (former deposition point) to a finer grain size with increasing distance from the deposition point, could be observed. Sulfide oxidation and the subsequent AMD formation induced the dissolution of primary carbonates and silicates, resulting in the formation of secondary minerals such as gypsum and siderite (Fig. 1F). Siderite is an often reported secondary mineral resulting form the interaction between acid solution and carbonates (Al et al., 2000; Paktunc et al., 2004) and was mainly encountered close to the contact with the Excelsior waste-rock dump and below the oxidation zone replacing primary dolomite in small fractures where the acid, iron-rich solution percolated (Fig. 1F).

In the 11 years after the operation ceased, the Quiulacocha tailings have developed an oxidation zone with a thickness between a few mm to a maximum of 25 cm, with pH ranging between 1.9 and 4.8. Areas with a very thin oxidation zone were characterized by cementation of the pore space by secondary minerals, giving the oxidation zone a hard and compact appearance, called the "cemented zone" (McGregor and Blowes, 2002). The mineralogy of the oxidation zone (Fig. 1B; Table 2) was characterized by an assemblage of residues of pyrite, quartz and secondary phases such as jarosite ($KFe_3(SO_4)_2(OH)_6$), gypsum ($CaSO_4.2H_2O$), relicts from primary siderite, and Fe(III) hydroxides, mainly goethite (confirmed by DXRD). The oxidation of sulfide minerals generated acid solutions and mobilized the associated metals (Fe, Cu, Zn, Pb). The interaction of these acid waters with the gangue minerals caused their dissolution and subsequent liberation of K^+, Na^+ and Ca^{2+}. These cations played a key role in the formation of secondary phases such as jarosite, gypsum, and siderite. Detailed sampling of the oxidation/primary zone interface have shown that the pH increased rapidly with depth from 1.9–2.5 in the oxidation zone (0–10 cm depth) up to 5–6 in 10–20 cm depth and to 7–8.3 in 1–1.5 m depth in the three drillings in the Zn–Pb tailings (CPQ/A, CPQ/B, CPQ/C; Table 3). This result indicates clearly that the carbonates (dolomite and siderite) associated to the Zn–Pb mineralogy were still able to buffer the acidity produced by sulfide oxidation in the oxidation zone.

In the oxidation zone, in the absence of cementation, O_2 and CO_2 concentrations at 15 cm depth were 13.4% and 2.54%, respectively. If a cemented zone was present, O_2 and CO_2 concentrations decreased to 9.80% and 0.94%, respectively. The formation of a cemented zone constituted a diffusion barrier for gases, limiting oxygen infiltration at greater depth (Blowes et al., 1991; McGregor and Blowes, 2002). This effect produced decreased oxidation kinetics, resulting in a thin oxidation zone. Our study suggests that in iron-rich systems (like pyrite-rich mine tailings, ~20–70% pyrite), secondary ferric minerals (such as jarosite or goethite), will form at lower pH because of ferric hydroxide's solubility is lower in these systems. This result is based on the control of the ferric hydroxide solubility, which decreases towards lower pH with higher concentrations, as is the case with all bi- and trivalent metal cations (Stumm and Morgan, 1996). The decrease in solubility of the ferric hydroxides decreases ferric ion mobility due to the initiation of in-situ hydrolysis and precipitation of Fe(III) hydroxides and the subsequent formation of a cemented zone. This also limits the more effective oxidation of metal sulfides via ferric iron, since it is fixed in the secondary phases. An often observed textural feature in these systems is the coating of sulfides (e.g. pyrite and pyrrhotite) by secondary ferric phases such as goethite, where this feature can be explained by the low mobility of ferric iron in high sulfide systems. In contrast, in low-iron systems, like the porphyry copper tailings (1–2 wt.% pyrite), the mobility of ferric iron is higher (Dold and Fontboté, 2001; Dold et al., 2005) due to the higher solubility based on lower ferric concentrations. Complexation and reduction processes can additionally increase the iron mobility in these systems (Dold et al., 2005). The data suggest that the parameters promoting the formation of a cemented zone in case of Quiulacocha are a combination of the high sulfide content, fine grain size, and the presence of carbonates.

3.3. Formation of a Fe–Zn–Pb acid plume

As mentioned above, in the three drill holes (CPQ/A, B, and C) immediately below the tailings surface (1 m depth, primary zone), the pH values varied between 5.5 and 8.3 (Tables 2 and 3). Therefore, the zone with acidic pH (5.6–6.1) and high metal concentrations in solution (Fe = 1262–7440 mg/L; Zn = 153–627 mg/L; Pb = 1.12–1.22 mg/L; Table 1) found at 10–13 m depth of the tailings stratigraphy cannot originate from the acid production and element liberation at the active oxidation zone. Additionally, the pH of the primary zone increased from 5.5 close to Excelsior (CPQ/A) to 7.5, increasing with the distance from the waste-rock dump Excelsior at CPQ/C. These observations suggest an infiltration of acid Fe(III)-rich waters from the waste-rock dump Excelsior towards the underlying Quiulacocha tailings impoundment. This AMD infiltration, which was produced by sulfide oxidation in the Excelsior waste-rock dump (Smuda et al., 2007), increased the oxidation processes by Fe(III) in the tailings by Eq. (1) (see also equations in Fig. 3) and reduced Fe(III) to Fe(II), explaining the formation of an acid Fe(II)–Zn–Pb plume in the carbonate containing Zn–Pb tailings (Fig. 3).

$$FeS_2 + 14Fe^{3+} + 8H_2O \rightarrow 15Fe^{2+} + 2SO_4^{2-} + 16H^+ \quad (1)$$

Data from sequential extraction support this interpretation, since they show that Zn is mainly enriched in the water-soluble and sulfide fraction at the depths where the Fe(II)–Zn–Pb plume was detected (e.g. CPQ/A 4.2 m, CPQ/B 9.5 and 11 m; Table 1). Lead is mainly associated to the NH_4-acetate leach (up to 4720 mg/kg in CPQ/B 11 m; Table 4) and the sulfide fraction, result suggesting that the most likely secondary anglesite ($PbSO_4$) was dissolved in the NH_4-acetate leach. There is no data available on the solubility of anglesite in NH_4-acetate or NH_4-oxalate solutions. However, the fact that in the NH_4-oxalate leach only 571 mg/kg Pb was present suggests that the anglesite might dissolve in the NH_4-acetate leach. The high concentration of Zn and Pb in the two upper samples of the AMD pond (CPQ/D 4.5 and 5.5 m) suggests an enrichment of these elements due to the constant AMD contribution from Excelsior, which then were retained as secondary sulfides or sulfates. Arsenic was mainly retained at CPQ/D in the fraction of secondary Fe(III)hydroxides (1050–1800 mg/kg). These Fe(III) hydroxides form when the Fe(III)-rich AMD from the Quiulacocha pond infiltrates into the underlying tailings, where

Please cite this article as: Dold, B., et al., Water management for acid mine drainage control at the polymetallic Zn–Pb–(Ag–Bi–Cu) deposit Cerro de Pasco, Peru, Journal of Geochemical Exploration (2008), doi:10.1016/j.gexplo.2008.05.002

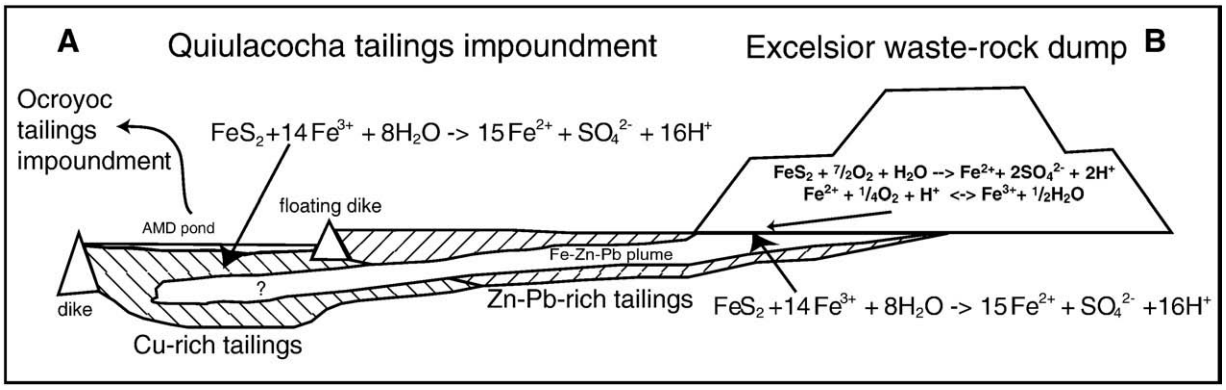

Fig. 3. Profile and relationships between AMD production in the Excelsior waste-rock dump and the export of Fe(III)-rich solution to the Quiulacocha tailings impoundment. The infiltration of Fe(III)-rich AMD enhanced the sulfide oxidation in Quiulacocha and the formation of a Fe(II)–Zn–Pb plume detected in the Zn–Pb-rich tailings. In the Cu-rich tailings, the overlying AMD pond enhanced the oxidation of this material and the liberation of the associated arsenic. The exportation of Fe(III)-rich AMD to Ocroyoc from the AMD pond at Quiulacocha, increased importantly sulfide oxidation in the active tailings impoundment.

the pH increased to 5.4 and the hydrolysis of the Fe(III)hydroxides was initiated.

3.4. Cu-sulfide tailings

The Cu-sulfide tailings were characterized by the association of pyrite–enargite–chalcopyrite–sphalerite–galena. Quartz was the dominant gangue mineral and is associated with aluminosilicates such as dickite/kaolinite as well as alunite. Primary carbonates (dolomite and siderite) were almost absent (Table 2). The Cu-sulfide tailings were deposited in the SW part of Quiulacocha, in the former natural lagoon of Quiulacocha underlying the Zn–Pb tailings in the central part of Quiulacocha (CPQ/C), which were separated by a floating dike (Fig. 2). In the particular acid conditions of the SW part of the tailings (near the AMD pond pH around 2.3), the oxidation of sulfide minerals such as enargite (Cu_3AsS_4) and chalcopyrite ($CuFeS_2$) caused the liberation of Cu and As. Cu was then leached downwards (low pH and reducing condition) where it replaced chalcopyrite by covellite (CuS; Fig. 1G), a process often reported from Cu-sulfide mine tailings (Dold and Fontboté, 2001). This process generated secondary enrichments with copper concentrations increasing from 1092 mg/kg (5.5 m depth) to 7225 mg/kg (9.5 m depth), from which an important part (1090 mg/kg Cu) was associated to the secondary Cu-sulfide fraction of the sequential extraction (Table 4). Additionally, as the Cu-rich tailings in the SW part of Quiulacocha (drilling CPQ/D), with a pH around 4.5, were influenced by AMD infiltration from the pond (pH = 2.3), the arsenic content in this pond remained high (6.54 mg/L) and constituted a main pollutant. The main sources of arsenic were enargite (Cu_3AsS_4), and to a lesser extent arsenopyrite (FeAsS) and tennantite ($Cu_{12}As_4S_{13}$). Thus, the Cu-rich tailings were also influenced by the AMD from the Excelsior waste-rock dump. Pumping of the Fe(III)-rich acid waters from the Quiulacocha pond in the active tailings impoundment Ocroyoc (Fig. 1D) represents also an export of acid potential, as indicated in Eq. (1), resulting in a drop of the pH in Ocroyoc and AMD formation in the active tailings impoundment (Fig. 1E).

4. Conclusion

The geochemical and mineralogical study of the Quiulacocha tailings impoundment has shown that the hydrological connection of the three mine-waste systems at Cerro de Pasco (Excelsior, Quiulacocha, Ocroyoc) is the most critical concern for waste management. During the historical exploitation of the Cerro de Pasco deposit, two distinct tailings types were exposed to oxidizing conditions and in contact with AMD, resulting in a very different geochemical behavior. The Zn–Pb-rich tailings of Quiulacocha did not release significant amounts of AMD to the system because the underlying carbonate-rich material of the oxidation zone was able to neutralize the acidity produced through sulfide oxidation. The main AMD source detected was the Excelsior waste-rock dump. Its acid seepage infiltrated into Quiulacocha, forming a Fe(II)–Zn–Pb plume (Fig. 3). The infiltration of Fe(III)-rich solutions resulted in enhanced acid production through pyrite oxidation (16 moles of protons per mole of pyrite oxidized; Eq. (1)) and also increased sulfide oxidation kinetics and dissolution in the Quiulacocha tailings. Although the carbonates were still able to neutralize the acidity produced in the oxidation zone, the additional input of Fe(III)-rich AMD from Excelsior exceeded the carbonates' buffer capacity of and resulted in the drop of pH to acid conditions (pH 5–6). The collection of Fe(III)-rich AMD emanating from the Excelsior waste-rock dump and transfer to the AMD pond of Quiulacocha increased the oxidation of the Cu-rich tailings in the SW part of the tailings impoundment and promoted liberation of arsenic from sulfide minerals such as enargite, arsenopyrite, and tennantite to the environment. The pumping of the Fe(III)-rich acid surface water from the Quiulacocha pond into the active Ocroyoc tailings also increased sulfide oxidation and acid production in the fresh alkaline tailings. The results suggest that a hydrological separation of the different mine-waste systems might be a first step to prevent further extension of the AMD problem. This study clearly shows that a main focus in acid mine drainage management must be the collection of the Fe(III)-rich AMD close to the source for treatment in order to prevent acid potential exportation through sulfide oxidation by Fe(III)-rich solutions (Eq. (1)).

Acknowledgements

We would like to thank the CENTROMIN management, Peru for their interest, support and access to their properties, especially Antonio Cornejo and Juana Rosa del Castillo. Special thanks are due to Volcan S.A.A for their logistic support and hospitality during the sampling campaign in 2003, especially Victor Gobitz, F. Grimaldo, Luis Osorio, and Walter Herredia and Antonio Samaniego from SVS Ingenieros, Lima, Peru for the flush drilling equipment. For analytical support we thank R. Martini, F. Capponi, A. de Haller, J.-M. Boccard, G. Overney, H.-R. Pfeifer, J.-C. Lavanchy at the University of Geneva and University of Lausanne, Switzerland. The project was organized with the support of Silvia Rosas (Pontificia Universidad Católica del Perú, Lima) and was financed by the Swiss Commission for Research Partnerships with Developing Countries (KFPE).

Please cite this article as: Dold, B., et al., Water management for acid mine drainage control at the polymetallic Zn–Pb–(Ag–Bi–Cu) deposit Cerro de Pasco, Peru, Journal of Geochemical Exploration (2008), doi:10.1016/j.gexplo.2008.05.002

References

Al, T.A., Martin, C.J., Blowes, D.W., 2000. Carbonate-mineral/water interactions in sulfide-rich mine tailings. Geochimica et Cosmochimica Acta 64, 3933–3948.

Baumgartner, R., 2007. Sources and evolution in space and time of hydrothermal fluids at the Cerro de Pasco Cordilleran base metal deposit, vol. 66. Terre & Environnement, Central Peru, p. 167.

Baumgartner, R., Fontboté, L., Vennemann, T., in press. Mineral zoning and geochemistry of epithermal polymetallic Zn-Pb-Ag-Cu-Bi mineralization at Cerro de Pasco, Peru. Economic Geology.

Blowes, D.W., Reardon, E.J., Jambor, J.L., Cherry, J.A., 1991. The formation and potential importance of cemented layers in inactive sulfide mine tailings. Geochimica et Cosmochimica Acta 55, 965–978.

Dold, B., 2003a. Dissolution kinetics of schwertmannite and ferrihydrite in oxidized mine samples and their detection by differential X-ray diffraction (DXRD). Applied Geochemistry 18, 1531–1540.

Dold, B., 2003b. Speciation of the most soluble phases in a sequential extraction procedure adapted for geochemical studies of copper sulfide mine waste. Journal of Geochemical Exploration 80, 55–68.

Dold, B., Fontboté, L., 2001. Element cycling and secondary mineralogy in porphyry copper tailings as a function of climate, primary mineralogy, and mineral processing. Special Issue: Geochemical studies of Mining and the Environment. Journal of Geochemical Exploration 74, 3–55.

Dold, B., Blowes, D.W., Dickhout, R., Spangenberg, J.E., Pfeifer, H.-R., 2005. Low molecular weight carboxylic acids in oxidizing porphyry copper tailings. Environmental Science and Technology 39, 2515–2521.

Einaudi, M.T., 1977. Environment of ore deposition at Cerro de Pasco, Peru. Economic Geology 72, 893–924.

Light, T.S., 1972. Standard solution for redox potential measurement. Analytical Chemistry 44, 1038–1039.

McGregor, R.G., Blowes, D.W., 2002. The physical, chemical and mineralogical properties of three cemented layers within sulfide-bearing mine tailings. Journal of Geochemical Exploration 76, 195–207.

Nordstrom, D.K., 1977. Thermochemical redox equilibria of Zobell's solution. Geochimica et Cosmochimica Acta 41, 1835–1841.

Nordstrom, D.K., 1982. Aqueous pyrite oxidation and the consequent formation of secondary iron minerals. In: Kittrick, J.A., Fanning, D.S. (Eds.), Acid Sulfate Weathering. Soil Sci. Soc. Am. J. , pp. 37–56.

Paktunc, D., Foster, A., Heald, S., Laflamme, G., 2004. Speciation and characterization of arsenic in gold ores and cyanidation tailings using X-ray absorption spectroscopy. Geochimica et Cosmochimica Acta 68, 969–983.

Patterson, R.J., Frape, S.K., Dykes, L.S., McLeod, R.A., 1978. A coring and squeezing technique for detailed study of subsurface water chemistry. Canadian Journal of Earth Sciences 15, 162–169.

Schippers, A., 2007. Microorganisms involved in bioleaching and nucleic acid–base molecular methods for their identification and quantification. In: Donati, E.R., Sand, W. (Eds.), Microbial Processing of Metal Sulfides. Springer, Dordrecht, pp. 3–34.

Singer, P.C., Stumm, W., 1970. Acid mine drainage: the rate-determining step. Science 167, 1121–1123.

Smuda, J., Spangenberg, J.E., Dold, B., 2006. Tracing water and dissolved sulfate sources in active mine tailings using S, H and O isotopes. Geochimica et Cosmochimica Acta 70, A601.

Smuda, J., Dold, B., Friese, K., Morgenstern, P., Glaesser, W., 2007. Mineralogical and geochemical study of element mobility at the sulfide-rich Excelsior waste rock dump from the polymetallic Zn–Pb–(Ag–Bi–Cu) deposit, Cerro de Pasco, Peru. Journal of Geochemical Exploration 92, 97–110.

Stumm, W., Morgan, J.J., 1996. Aquatic Chemistry. Wiley, New York.

Wisskirchen, C., Dold, B., Friese, K., Morgenstern, Gläser, W., 2005. Hydrogeochemistry and sediment mineralogy of the extremely acidic mine water lagoon Yanamate at the Pb–Zn deposit Cerro de Pasco, Peru. Securing the Future 2005, International Conference on Mining and Environment and Metals and Energy Recovery, Skelleftea, Sweden, pp. 1013–1022.

Please cite this article as: Dold, B., et al., Water management for acid mine drainage control at the polymetallic Zn–Pb–(Ag–Bi–Cu) deposit Cerro de Pasco, Peru, Journal of Geochemical Exploration (2008), doi:10.1016/j.gexplo.2008.05.002